applied sciences

Article

Technoeconomic Analysis of Oxygen-Supported Combined Systems for Recovering Waste Heat in an Iron-Steel Facility

Busra Besevli [1], Erhan Kayabasi [2,3,*], Abdulrazzak Akroot [2,*], Wadah Talal [2], Ali Alfaris [2], Younus Hamoudi Assaf [2], Mohammed Y. Nawaf [2], Mothana Bdaiwi [2] and Jawad Khudhur [2]

1 Property Protection and Security Department, TOBB Technical Sciences Vocational School, Karabuk University, 78050 Karabuk, Türkiye; busrabesevli@karabuk.edu.tr
2 Mechanical Engineering Department, Engineering Faculty, Karabuk University, 78050 Karabuk, Türkiye; eng.wadah26@gmail.com (W.T.); ali75f@gmail.com (A.A.); younisassaf2020@gmail.com (Y.H.A.); mohmax977@gmail.com (M.Y.N.); mothna777@gmail.com (M.B.); jawdyahya5@gmail.com (J.K.)
3 Iron Steel Institute, Karabuk University, 78050 Karabuk, Türkiye
* Correspondence: erhankayabasi@karabuk.edu.tr (E.K.); abdulrazzakakkroot@karabuk.edu.tr (A.A.)

Abstract: In this study, it is proposed to generate electrical energy by recovering the waste heat of an annealing furnace (AF) in an iron and steel plant using combined cycles such as steam Rankine cycle (SRC), organic Rankine cycle (ORC), Kalina cycle (KC) and transcritical CO_2 cycle (t-CO_2). Instead of releasing the waste heat into the atmosphere, the waste heat recovery system (WHRS) discharges the waste heat into the plant's low-temperature oxygen line for the first time, achieving a lower temperature and pressure in the condenser than conventional systems. The waste heat of the flue gas (FG) with a temperature of 1093.15 K from the reheat furnace was evaluated using four different cycles. To maximize power generation, the SRC input temperature of the proposed system was studied parametrically. The cycles were analyzed based on thermal efficiency and net output power. The difference in SRC inlet temperature is 221.6 K for maximum power output. The proposed system currently has a thermal efficiency and total power output of 0.19 and 596.6 kW, respectively. As an environmental impact, an emission reduction potential of 23.16 tons/day was achieved. In addition, the minimum power generation cost of the proposed system is $0.1972 per kWh.

Keywords: waste heat recovery; steam Rankine cycle; organic Rankine cycle; CO_2 cycle; Kalina cycle; thermal analysis

Citation: Besevli, B.; Kayabasi, E.; Akroot, A.; Talal, W.; Alfaris, A.; Assaf, Y.H.; Nawaf, M.Y.; Bdaiwi, M.; Khudhur, J. Technoeconomic Analysis of Oxygen-Supported Combined Systems for Recovering Waste Heat in an Iron-Steel Facility. *Appl. Sci.* **2024**, *14*, 2563. https://doi.org/10.3390/app14062563

Academic Editor: Anna Stoppato

Received: 14 February 2024
Revised: 4 March 2024
Accepted: 6 March 2024
Published: 19 March 2024

1. Introduction

Although the iron and steel industry has made significant progress in recent years, it still has a potential of reduction of approximately 20% in energy consumption and emission generation depending on high fossil fuel consumption [1,2]. Wasted thermal energy at 800–900 °C from conventional iron and steel factories has promising potential for electricity generation using various energy conversion methods [3]. In addition, it will reduce CO_2 emissions and increase overall efficiency. Waste heat recovery systems (WHRS), which are essential applications for strategic energy distribution, can significantly reduce energy consumption and emissions. Depending on the temperature level, waste heat sources can be divided into three categories such as low-grade waste heat (less than 230 °C), medium-level waste heat (between 230 and 650 °C) and high-grade waste heat (more than 650 °C) [4–6]. In this context, waste heat must be converted using appropriate energy conversion systems considering temperature ranges. This situation necessitates the use of multiple and sequential systems for energy conversion [7,8]. The temperature ranges of the systems vary according to the type of working fluid in the systems, the investment costs, the size of the equipment used in the systems and the economic ranges of the electricity generation costs. In addition, the efficiency ranges of the systems and the combined thermal efficiencies should also be considered. Therefore, to minimize energy production costs, determining the operating temperature ranges of the systems, optimizing the equipment dimensions, and investment costs, power outputs and thermal efficiency are among the intensively studied subjects today.

Various methods can be used for waste heat recovery methods, such as steam Rankine cycle (SRC), Kalina cycle (KC), organic Rankine cycle (ORC), Brayton cycle (BC) and CO_2 cycle. Depending on the operating conditions, such as temperature, pressure, mass flow rate and type of heat source, combined systems are intensively employed in recovering heat from waste heat to generate electricity and decrease fuel consumption and emissions [9]. For instance, Ozcan et al. [10] aimed to produce synthetic fuel by hydrogenating captured CO_2 using moderate waste heat rejected from an iron and steel production facility and investigated its thermodynamic and economic feasibility. They used the KC to generate electricity and provide heat from the CO_2 capture plant (CCP). The electricity generated from the systems was used by the PEM electrolyzer and all power-consuming components of the facility. KC showed the highest efficiency at a 488 °C turbine inlet temperature and 65% ammonia fraction. The facility's fuel production efficiency reached 19% at the cost of 532 $/tons methanol. Lu et al. [11] developed a new WHRS in their studies. They used the Rankine systems to generate power from slag waste heat, using a high level of waste heat, and used ORC and absorption refrigeration systems for gradual heat recovery; they also made a thermodynamic, thermoeconomic and environmental analysis of the facility they designed and tried different working fluids that can be environmentally friendly for the ORC systems. As a result of their work, a significant amount of electricity has been produced from ORC. The energy efficiency of the facility was calculated as 37.66%. Ishaq et al. [12] presented an integrated system design for hydrogen production at high pressure by utilizing steel furnace waste heat in their studies. The integrated system consists of a hydrogen compression system and a copper chlorine system. They obtained the electrical energy required for the system from the Rankine cycle and simulated the system with ASPEN Plus V9. Energy and exergy efficiencies were calculated as 38.2% and 39.8%, respectively. Ma et al. [13] evaluated the recovery and use of the waste heat of an iron and steel production plant according to the quality of the waste heat. As a result of their studies, it was stated that the low-temperature waste heat generated in the facility was not used, and it should be used in the future. It is noted that waste heat recovery is relatively low in the section where coking and sintering processes are located in the facility. They stated that the use of waste heat should be in accordance with the first and second law of thermodynamics and recovery methods corresponding to the quality of waste heat should be used. An innovative technoeconomic model was created by Qi Zhang et al. [14] for the recycling of waste energy. To evaluate falling energy use and anticipated future energy savings, they built up a number of scenarios. It is evident from their findings that there is less than a 20% chance of energy savings. Waste energy recycling's most critical parameters have been identified. It has been shown that the techno-economic approach they use allows for the recovery of about 44% of the waste heat. However, there has not been much research done on the various energy conversion systems that span large temperature ranges in iron and steel plants to recover FG thermal energy into electrical power.

In this study, in order to generate electricity from high-temperature FG heat discharged from an industrial annealing furnace (AF), sequential thermodynamics was applied employing the low-temperature O_2 line established for using the oxygen-enriched combustion processes in the facility for the first time in order to reach lower temperature and pressure in condensers. Firstly, the RC and the t-CO_2 cycle were used together. Afterwards, the FG was released to the atmosphere at low temperatures using ORC and KC in the system, respectively. In the last stage, the low-temperature O_2 line, which is produced to enrich the combustion processes in other departments of the factory, was evaluated as a heat resource in the condensers of the cycles.

2. Materials and Methods

This study focuses on the evaluation of waste heat of an AF. Within the scope of the study, the efficiency of the system was increased by designing a combined system in order to generate electricity by using the waste heat from the AF and to reduce the FG emissions released into the atmosphere.

2.1. System Design

The FG rejected from the AF at a temperature of 1093.15K transfers its heat to the RC evaporator through HX1 (point a). In the RC, water is compressed in the pump from 369.5 K and 0.7 bar to 373.18 K and 150 bar. Afterwards, it is heated to 873 K with the heat recovered from the FG in the evaporator and transitions to the superheated vapor phase. The superheated steam exits as a saturated liquid at 369.5 K and 0.7 bar through the intermediate heated turbine. Afterwards, the condensation energy in the RC condenser is transferred to the CO_2 cycle at constant pressure. Afterwards, the FG enters the ORC evaporator (HX3) at 661.4 K (point b). R245fa is used as the working fluid in ORC, is compressed from 298 K 1.5 bar to 299 K 20 bar in the pump. Afterwards, it is heated to 435 K using the heat recovered from the FG in the ORC evaporator. In the superheated vapor phase, R245fa expands in the turbine to 416 K and 1.5 bar. Afterwards, it is cooled at 298 K at constant pressure in the ORC condenser. FG enters the KC evaporator at 461 K (HX4) and transfers its waste heat to the ammonia water mixture.

The working fluid of the KC is a binary combination of ammonia and water that goes through a special mechanism to change the ammonia content all throughout the system. Heat recovery efficiency is greatly increased by this procedure. The addition of ammonia permits boiling at lower temperatures, allowing for the effective use of waste heat. After that, a heat exchanger (HX4) is used to transfer the energy from flue gas remaining to the binary working fluid (NH_3-H_2O mixture) of the KC. The energy that is produced is then used to power the KC, which generates electricity using standard methods.

The pump, separator, turbine, regenerator, expansion valve, mixer, condenser, and steam generator are the essential parts of the KC, as shown in Figure 1. At state point 17, the NH_3-H_2O combination's liquid and vapor mixture enter the separator. The separator's job is to fully separate the vapor and liquid; at state point 18, which is the turbine entry, the mixture bifurcates into a rich combination of NH_3-H_2O and a lean mixture at state 20. In order to generate power, the turbine expands the rich NH_3-H_2O combination to a low condensation pressure. The rich mixture from the turbine discharge enters the mixer at state point 19, while the weak mixture of NH_3-H_2O exiting the separator (state 20) passes through the regenerator, where it releases energy into the NH_3-H_2O mixture's basic solution. The basic solution then enters the heat recovery vapor generator (HX4) at state point 17. At state point 21, the weak combination then experiences a decrease in temperature. Allowing the weak mixture to expand through the valve lowers its temperature even more (state 24). The rich mixture and weak mixture combine in the mixer to create the high-energy basic solution of the NH_3-H_2O combination (State 22). The condenser is now subjected to the high energy basic solution, which discharges at state 23 (HX6). At state 16, the condensed NH_3-H_2O combination is pumped to the vapor generator. The ammonia-water mixture's temperature, pressure, and concentration at the turbine's inlet are all kept constant during the KC. By doing this, the steady heat input required to keep the KC running is guaranteed. By modifying the mass flow rate of the NH_3-H_2O mixture in the KC, variations in the amount of heat delivered by the FG are offset. Finally, all cycles release their waste heat using C1, C2, and C3 to the pure oxygen line, which is used to enrich the oxygen available in the factory. Using the Engineering Equation Solver (EES V10 561 3D), a mathematical model is created to examine the integration of waste heat and the power cycles [15]. The optimization goal can be well-explained by decreasing the flue gas emissions and waste heat rate and maximizing the thermal efficiency with minimum electricity cost. Here the main purpose is to benefit from the high temperature flue gas as possible and decreasing the fuel consumption and CO_2 emissions. For this purpose, the parameters resulting in the minimum electricity cost were selected for the optimum point.

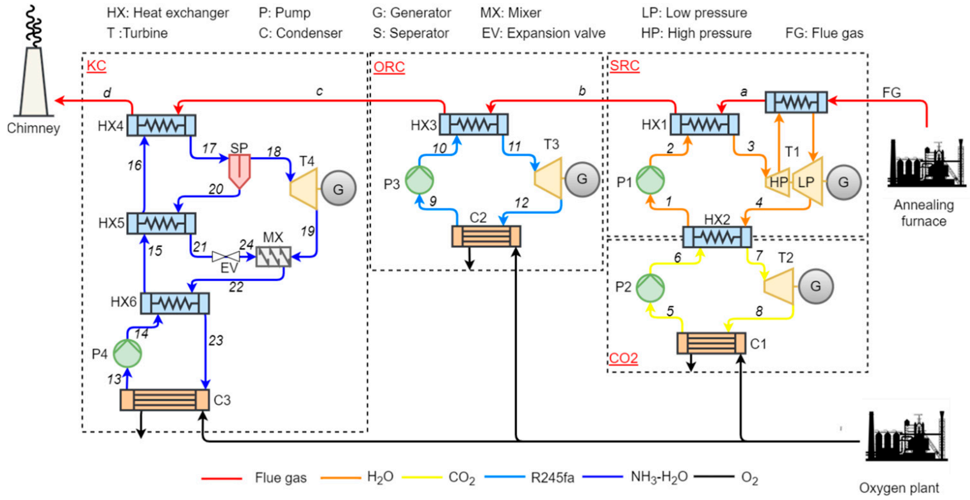

Figure 1. General layout of the cascaded WHRS by the numbers of stations from 1–24 for the cycle components and by the letters from a–d for the stations of flue gas.

Combined systems have been designed and optimized for the recovery of FG waste heat from the AF. It aims to improve the system's efficiency, generate electricity, and reduce the emission of FG to the atmosphere in an attractive way. The FG properties are listed in Table 1.

Table 1. Flue gas thermophysical properties.

Parameter	Value	Unit
Outlet temperature	1093.15	K
Volumetric flow rate	40,000	m^3/h
Density	0.3027	kg/m^3
Specific heat	1.382	kJ/kgK
Pressure	1	atm

By analyzing the mass flow rate parametrically, alterations have been investigated on the systems' thermal efficiency, net power, and electricity generation cost. Effectiveness values for heat exchangers (HX) and pump pressure ratio of CO_2 cycle are considered 0.8 [16] and 0.1 [10] respectively.

2.2. Thermodynamic Model

Energy calculations were performed to impart the systems that provide the minimum electricity production cost considering the first law of thermodynamics. First, FG density and specific heat values are calculated using EES according to FG elemental content and fractions.

Energy and mass balance equations are provided as in Equations (1) and (2) [17]:

$$\sum \dot{m}_{in} = \sum \dot{m}_{out} \tag{1}$$

$$\dot{Q} + \dot{W} = \sum \dot{m}_{out} h_{out} - \sum \dot{m}_{in} h_{in} \tag{2}$$

$\dot{Q}$ and $\dot{W}$ refer to heat transfer rate and work leaving control volume [18], respectively. $\dot{m}$ refers to mass flowrates of the flows, and the indices stand for the inlet and the outlets.

$$\dot{W}_{net} = \dot{W}_t - \dot{W}_p \tag{3}$$

where $\dot{W}_{net}$ stands for each system's net power, $\dot{W}_t$ indicates output power of turbine, and $\dot{W}_p$ is the required pump power.

The thermal efficiency is calculated using Equation (4) [19]:

$$\eta_{th} = \frac{\dot{W}_{net}}{\dot{Q}_{in}} \quad (4)$$

Turbine efficiency of SRC, ORC, and CO_2 is calculated by [11]:

$$\eta_{th,src} = \frac{h_3 - h_{4a}}{h_3 - h_{4s}} \quad (5)$$

Here, h indicates the enthalpy values of the flows, and subscript a indicates the actual values. Turbine efficiency of ORC is calculated by

$$\eta_{th,orc} = \frac{h_7 - h_{8a}}{h_7 - h_{8s}} \quad (6)$$

Turbine efficiency of CO_2 is calculated by

$$\eta_{th,CO_2} = \frac{h_{11} - h_{12a}}{h_{11} - h_{12s}} \quad (7)$$

where $\dot{Q}_{in}$ is rate of thermal energy provided by FG. Table 2 represents energy balance equations for the components of each system.

Table 2. Energy balance equations [12].

Cycle	Component	Equation
SRC	Steam turbine	$\dot{W}_{t,SRC} = \dot{m}_{SRC}(h_3 - h_4)$
	Condenser	$\dot{m}_{SRC}(h_4 - h_1) = \dot{m}_{CO2}(h_7 - h_6)$
	Water pump	$\dot{W}_{p,SRC} = \dot{m}_{SRC}(h_2 - h_1)$
	Evaporator	$\dot{m}_{SRC}(h_3 - h_2) = \varepsilon_{Hex}\dot{m}_{fg}C_{p,fg}(T_a - T_b)$
CO_2	Turbine	$\dot{W}_{t,CO2} = \dot{m}_{CO2}(h_7 - h_8)$
	Condenser	$\dot{m}_{CO2}(h_8 - h_5) = \dot{m}_{oxygen}(h_{II} - h_I)$
	Pump	$\dot{W}_{p,CO2} = \dot{m}_{CO2}(h_6 - h_5)$
ORC	Turbine	$\dot{W}_{t,ORC} = \dot{m}_{ORC}(h_{11} - h_{12})$
	Condenser	$\dot{m}_{ORC}(h_{12} - h_9) = \dot{m}_{oxygen}(h_{IV} - h_{III})$
	Pump	$\dot{W}_{p,ORC} = \dot{m}_{ORC}(h_{10} - h_9)$
	Evaporator	$\dot{m}_{ORC}(h_{11} - h_{10}) = \varepsilon_{Hex}\dot{m}_{fg}C_{p,fg}(T_b - T_c)$
KC	Turbine	$\dot{W}_{t,Kalina} = \dot{m}_{18}(h_{18} - h_{19})$
	Condenser	$\dot{m}_{23}(h_{23} - h_{13}) = \dot{m}_{oxygen}(h_{VI} - h_V)$
	Pump	$\dot{W}_{p,Kalina} = \dot{m}_{13}(h_{14} - h_{13})$
	Evaporator	$\dot{m}_{17}(h_{17} - h_{16}) = \varepsilon_{Hex}\dot{m}_{fg}C_{p,fg}(T_c - T_d)$
	Mixer	$\dot{m}_{19}h_{19} + \dot{m}_{24}h_{24} = \dot{m}_{22}h_{22}$
	Expansion valve	$h_{21} = h_{24}$
	LTR	$\dot{m}_{14}h_{14} + \dot{m}_{22}h_{22} = \dot{m}_{15}h_{15} + \dot{m}_{23}h_{23}$
	HTR	$\dot{m}_{15}h_{15} + \dot{m}_{20}h_{20} = \dot{m}_{16}h_{16} + \dot{m}_{21}h_{21}$

2.3. Techno-Economic Model

Maintenance cost, interest rates, and annual operating time were considered for the economic analysis. Given that each component in a process is anticipated to run during a specific timeframe, the capital cost rate expressed in \$/s is denoted by $\dot{Z}$ and can be found in Equation (8) [20].

$$\dot{Z} = \frac{PEC\phi CRF}{3600N} \quad (8)$$

Here, PEC, ϕ, CRF, and N are the purchased equipment cost, maintenance factor, the capital recovery factor, and the operation duration per year, respectively.

The maintenance factor is considered as 1.12, and the CRF is given as in Equation (9) [21]:

$$CRF = \frac{\iota(1+\iota)^n}{(1+\iota)^n - 1} \tag{9}$$

Interest rate (ι) and system life (n) were accepted as 10% and 30 years. Electricity product cost is calculated for each combined system in Equation (10) [10].

$$\dot{Z}_{elec} = \frac{\sum \dot{Z}_k}{\dot{W}_{net}} 3600 \tag{10}$$

$\dot{Z}_k$ indicates the total cost rate of systems. The subscript stands for the component number.

HXs in all systems were modeled using the following Equation (11) [17].

$$\dot{Q} = U_k A_k \Delta(T_m)_{ln} \tag{11}$$

Here, $\dot{Q}$ is the heat transfer rate across the heat exchangers, U is the overall heat transfer coefficient, and A is the heat transfer surface area of HX. $(\Delta T_m)_{ln}$ stands for the logarithmic mean temperature difference and can be calculated using Equation (12).

$$(\Delta T_m)_{ln} = \frac{(T_{h,i} - T_{c,o}) - (T_{h,o} - T_{c,i})}{\mathrm{In}\frac{(T_{h,i} - T_{c,o})}{(T_{h,o} - T_{c,i})}} \tag{12}$$

Here, T is the temperature of the flows, subscripts h and c indicate the hot flows and cold flows, and i and o indicate inlet and outlet, respectively. Table 3 gives the offered overall heat transfer coefficient values for the heat exchangers of the combined systems [22–24].

Table 3. Offered overall heat transfer coefficient values.

Heat Exchanger	U (kW/m^2K)	Ref.
H1	0.25	[22]
H2	1.6	[24]
H3	0.3	[23]
C1	1.6	[24]
C2	1.6	[24]

All combustion sources' emissions are calculated using fuel and the average emission factor. As shown in Equation (13) the C emissions component from coal was computed using the IPCC Tier 1 (1996) technique [25].

$$C_C = 32.15 - (0.234 \times H_V) \tag{13}$$

When considering Turkey, the calorific value of coal ranges from 33.49 TJ/kiloton to 37 TJ/kiloton on a dry mineral matter-free basis. C_c is the carbon emissions factor in t C/TJ; H_V is the gross calorific value of coal. Using Equations (14) and (15), the emissions from carbon and carbon dioxide are computed [26].

$$\text{Emissions}_C = C_C \times Q_{daily} \tag{14}$$

$$\text{Emissions}_{CO2} = \text{Emissions}_C \times 3.667 \tag{15}$$

The cost functions' essential correlations in the preliminary design stage are listed in Table 4.

Table 4. Purchase equipment costs for components.

Cycle	Component	Correlation	Explanation	Ref.
SRC	steam turbine	$PEC_{ST,SRC} = 4405\dot{W}_{ST}^{0.7}$	-	[27]
	condenser	$PEC_{cond,SRC} = 588A_{Cond}^{0.8}$	$A_{Cond} = Q/U(\Delta Tm)_{ln}$	[28]
	pump	$PEC_{wp,SRC} = 1120\dot{W}_P^{0.8}$	-	[23]
	evaporator	$PEC_{eva,SRC} = 6570\left(\frac{Q}{\Delta Tm}\right)^{0.8} + 21276\dot{m}_{src} + 1184.4\dot{m}_{fg}$	Q: heat transfer from flue gas ΔTm: Logaritmic mean temperature difference	[28]
CO_2	turbine	$PEC_{turbine,CO_2} = 866.64\dot{W}_T^{0.82}$	-	[29]
	condenser	$PEC_{cond,CO_2} = 2143A_{Cond}^{0.514}$	-	[29]
	pump	$PEC_{pump,CO_2} = 1120\dot{W}_P^{0.8}$	-	[29]
ORC	turbine	$PEC_{turbine,ORC} = 4750\dot{W}_t^{0.75}$	-	[28]
	condenser	$PEC_{cond,ORC} = 516.62A_{cond}^{0.6}$	-	[28]
	pump	$PEC_{pump,ORC} = 200\dot{W}_P^{0.65}$	-	[24]
	evaporator	$PEC_{eva,ORC} = 309.14A_{eva}^{0.85}$	-	[28]
KC	pump	$PEC_{pump,kalina} = 1120\dot{W}_P^{0.7}$	-	[30]
	condenser	$PEC_{cond,kalina} = 516.62A_{cond}^{0.6}$	-	[30]
	turbine	$PEC_{turbine,kalina} = 6000\dot{W}_t^{0.7}$	-	[30]
	separator	$PEC_{sep,kalina} = 114.5m^{0.67}$	-	[10]
	HTR, LTR	$PEC_{HTR,LTR,kalina} = 130\left(\frac{A_{hx}}{0.093}\right)^{0.78}$	-	[10]
	mixer	$PEC_{mix,kalina} = 114.5m^{0.67}$	-	[30]

2.4. Assumptions

In this study, the recovery of waste heat from a reheating furnace located in an iron and steel factory was studied. It is assumed that there is no heat loss in the fluid pipelines during the transfer of waste heat to the cycles and between the components. Effectiveness values for heat exchangers are stated in the relevant tables. Turbines and compressors in the cycles are considered isentropic. It is accepted that the liquids in the mixing chambers are completely mixed together. It is also known that the iron and steel factory is operated 360 days a year. The effective life of the designed system is planned to be 30 years, and the discount rate is 15%.

3. Results and Discussion

The goal of this project is to use coupled cycles to recover the waste heat in an FG from an industrial furnace. In SRC, ORC, and KC, respectively, FG was used to produce electrical energy. The FG temperature employed in the SRC was investigated parametrically in order to maximize the waste heat of FG in the cycles. The optimal point was determined to be the one that resulted in the lowest cost of producing electricity. Analysis was done on the net power production for each cycle ($\dot{W}_{net}$), thermal efficiency (η_{th}), and the cost of producing electricity ($\dot{Z}_{electricity}$). Additionally, energy balances were constructed, heat recovery potentials were disclosed, and relevant computations were performed utilizing the measurement data of the FG from the AF. The findings of parametric studies and the results computed using constant data for each coupled system are presented below, section by section.

Figure 2 represents the T−s diagram of SRC considering the optimum mass flowrate. As seen in the T−s diagram of SRC, the working fluid enters the pump as a saturated liquid at 0.6 bar pressure and 369.5 K temperature and is compressed at 150 bar pressure in the pump. It is assumed that the pump and turbine are isentropic. Using the heat taken from the FG, the temperature is increased to 873 K and expanded to 30 bar and 660 K in the high-pressure turbine. Afterwards, the temperature is increased to 873 K at constant pressure by applying reheating. In the low-pressure turbine, the working fluid expands to the condenser pressure of 0.6 bar and 369.5 K. Finally, saturated liquid is obtained in the condenser and heat rejected into the CO_2 cycle.

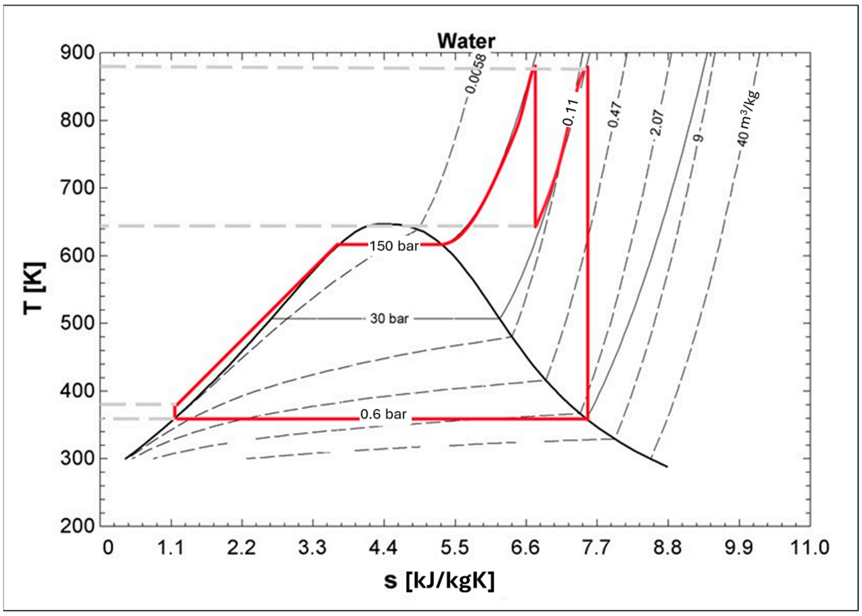

Figure 2. T−s diagram of SRC.

In the T−s diagram of CO_2, the working fluid enters the condenser as a saturated liquid at 233.028 K at a pressure of 10 bar as indicated in Figure 3. The CO_2 pressure rises to 90 bar, which is the condenser pressure in the pump. It is assumed that the pump and turbine are isentropic. The fluid temperature is increased to 359.5 K before the turbine inlet by using the heat released from the condenser of the SRC. The cycle is supercritical because the phase change takes place above the saturation curve. In the CO_2 turbine, the fluid expands to 233,028 K and 10 bar. The cycle is completed by heat rejection in the condenser to the oxygen line at constant pressure.

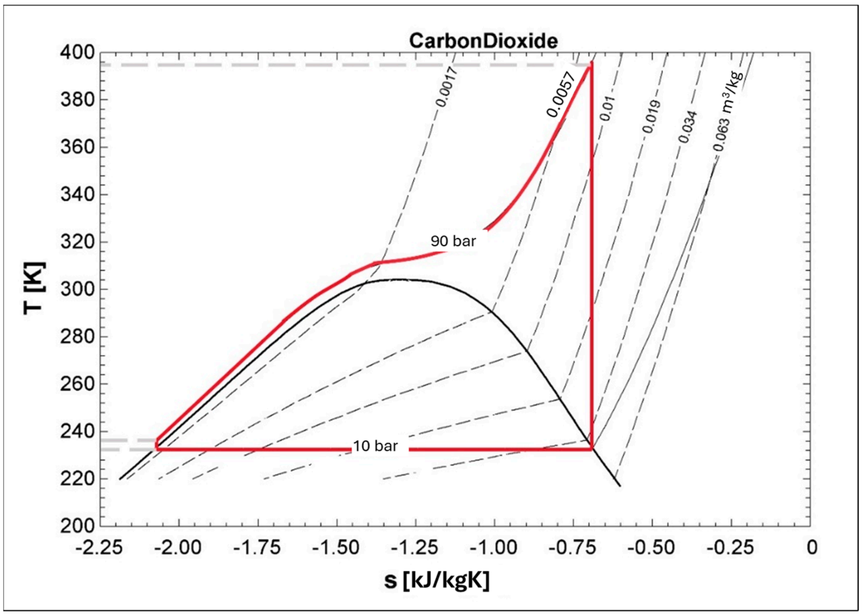

Figure 3. T−s diagram of CO_2 cycle.

As it is clearly observed in Figure 4, R245fa enters the pump as a saturated liquid at a temperature of 299.184 K and a pressure of 1.5 bar. The pressure of the working fluid in the pump is compressed to 20 bar. It is assumed that the pump and turbine in the cycle are isentropic. An amount of 865 kW of thermal energy from the FG was used to increase the temperature of the fluid. The temperature of the fluid after the evaporator is 435 K. In the turbine, the fluid expands to the condenser pressure. Finally, the fluid at 200 K temperature is condensed and the cycle is completed.

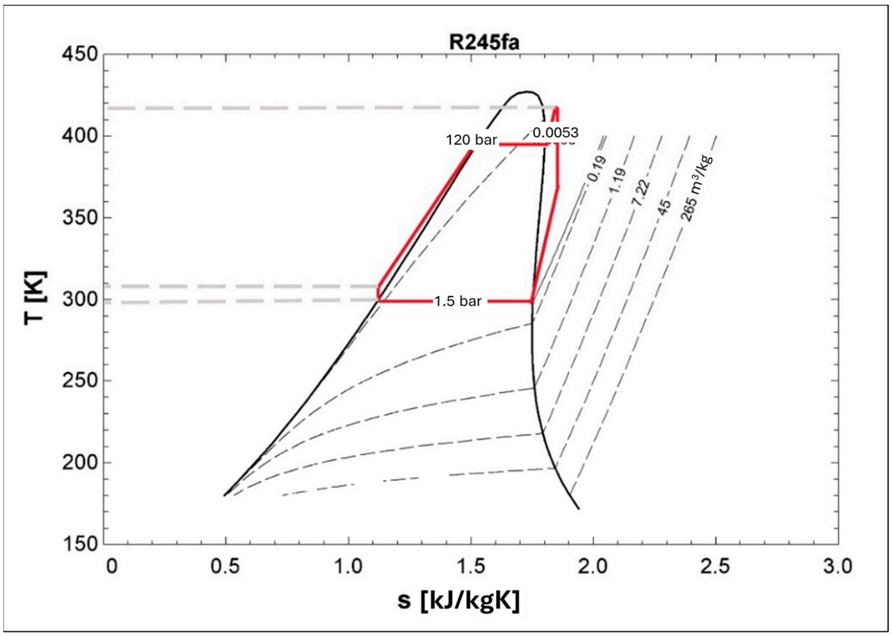

Figure 4. T−s diagram of ORC.

Figure 2 depicts a schematic of energy flows that illustrates potential interconnections between the district-level gas, heat, and electricity networks. Because of the close connections between the networks, oxygen, and electricity, an integration analysis is necessary to represent the heat HX networks. Any type of energy conversion component should be able to be included in the model, and it should be able to evaluate how it affects the technical functioning, flows, and losses of every network. In the end, this would also enable the computation of energy costs, carbon emissions, and energy efficiency in addition to a Sankey diagram depicting the energy flows over several networks under various circumstances.

According to the Sankey diagram in Figure 5, it is seen that 610 kW of the 3006.5 kW thermal energy of the FG can be recovered as electrical energy. In addition, it is observed that a total of 854 kW of thermal energy is wasted into the atmosphere from the HXs. It turns out that 1048 kW of thermal energy is transferred to the oxygen line to be used in the combustion processes that require enrichment with oxygen in other units in the facility. While there is 766.62 kW of thermal energy to produce a network in the SRC, this value has increased to 1535.23 kW thanks to the application of reheating, resulting in a network generated of 337.2 kW. In the proposed system, FG thermal energy was used first in SRC, then in ORC, and finally in KC, according to temperature classification. It is thought that a significant amount of thermal energy thrown into the atmosphere from the HXs in this system can be used in various industrial applications according to the temperature classification.

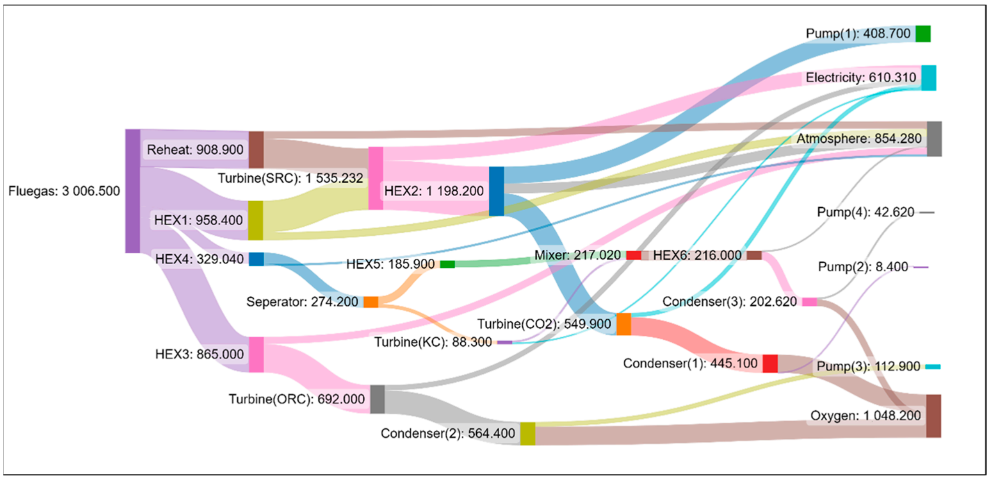

Figure 5. Schematic energy flow in the system.

To observe system reaction in relation to pressure, temperature, and mass flowrate, thermal analysis is necessary. This part presents the optimization of the proposed system, including the net power production determined by temperature difference, the total system thermal efficiency, and the costs associated with energy generation. Table 5 presents the values derived from the combined cycles as a consequence of the parametric analysis.

Table 5. Mass and energy balance of the proposed system.

Stream	T [K]	P [bar]	h [kJ/kg]	S [kJ/kgK]	$\dot{m}$ [kg/s]
1	883.000	0.7069	403.8	1.266	0.2424
2	369.500	150	419.3	1.296	0.2424
3	373.185	150	3583	6.679	0.2424
4	873.000	0.70	2672	7.51	0.2424
5	369.500	10	−394.1	−2.074	1.182
6	233.028	90	−387	−2.074	1.182
7	235.936	90	−14.95	−0.8276	1.182
8	359.500	10	−103.6	−0.8276	1.182
9	233.028	1.5	233	1.115	2.255
10	298.550	20	234.4	1.115	2.255
11	299.184	20	541.3	1.935	2.255
12	435.000	1.5	483.3	1.935	2.255
13	416.875	6	−92.98	0.26	0.2177
14	299.563	60	−85.93	0.26	0.2177
15	300.160	60	71.22	0.7558	0.2177
16	334.178	60	146.9	0.977	0.2177
17	350.000	60	1154	3.426	0.2177
18	450.000	60	1679	4.625	0.1107
19	450.000	6	1311	4.625	0.1107
20	348.496	60	611.7	2.186	0.107
21	450.000	60	349.7	1.569	0.107
22	400.000	6	838.6	3.159	0.2177
23	350.919	6	642.2	2.589	0.2177
24	335.919	6	349.7	1.641	0.107

Seyyedvalilu et al. (2021) provide a reference for determining turbine inlet temperature (TIT) and SRC pressure. For the SRC, the mass flow rate is determined to be 0.24 kg/s, while the TIT is 873 K, and its pressure is 150 bar. The mass flow rate resulted in a 333.5 kW SRC net power output. The SRC's working fluid has a turbine output temperature of 369.5 K and a pressure of 0.7 bar [29]. Based on these parameters, the temperature at the boiler entrance was determined. The fluid enters the boiler with a steam quality of x = 0. There is a constant pressure heat intake in the SRC evaporator.

EES was used to determine the thermodynamic parameters (enthalpy, entropy, and specific volume) based on this input data. Operating under the current conditions, SRC produces turbines with an output power of 337.2 kW and an efficiency of 0.34. Every SRC component's equipment acquisition cost was determined. The SRC provides power at a unit cost of 0.01592 $/kWh.

The SRC's condenser generates heat that is meant to be recovered via the CO_2 cycle as cascade heat. The CO_2 is saturated liquid (x = 0) and at CO_2 condenser with an outlet pressure of 10 bar. Values from the literature review were used to get the CO_2 cycle pressure value. Similar to the SRC, the pump work and condenser outlet enthalpy in the CO_2 cycle were used to compute the pump outlet enthalpy. The literature states that the turbine output power was computed using input parameters and the CO_2 cycle TIT. The combined system has a net output power of 429.83 kW. The suggested devices' ability to transfer heat from the FG depends critically on the mass flow rate.

Mass flow rate in a cycle is an important parameter during designing cycles, as it will directly affect the size and the cost of the components. In addition, since the heat transferred to the working fluid in the evaporator is directly related to the temperature, the relationship between temperature and mass flow gives important ideas about the power that can be obtained from the cycle. Therefore, when Figures 6 and 7 are examined together, it is seen that the curves of the mass flow rate and the heat transferred to the system are compatible with each other.

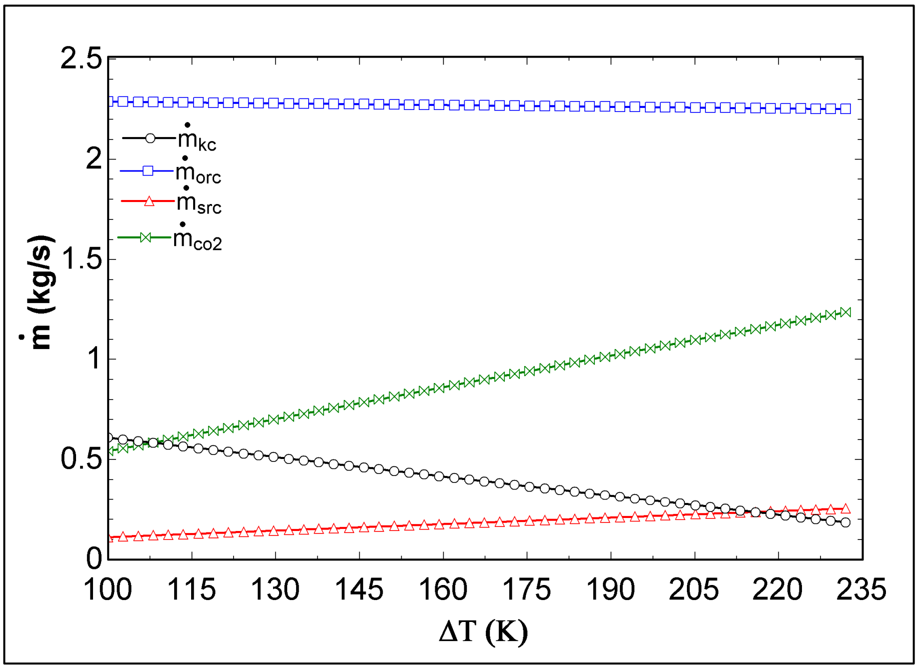

Figure 6. Change in mass flow rate with temperature difference.

Since the quality of the heat depends on the temperature, it is an easier method to work with SRC at high temperatures and to study the mass flow rate parametrically depending on the work output in the SRC to achieve maximum power generation. Thus, the total power generation continued to increase linearly, although the temperature increases in the SRC evaporator decreased the power generation in the ORC and KC as depicted Figure 8. The power generation of the CO_2 cycle increases due to the increase in the amount of heat removed from the SRC. However, the power generation in ORC and KC decreases linearly due to the transfer of heat at high temperatures to the SRC and CO_2 cycle.

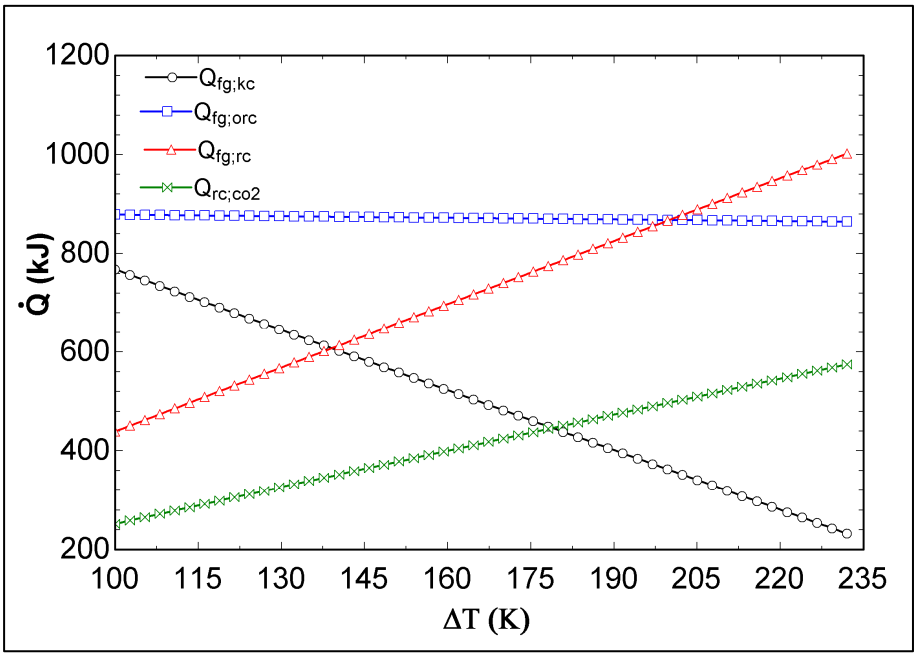

Figure 7. Heat distribution in the cycles according to the changing temperatures.

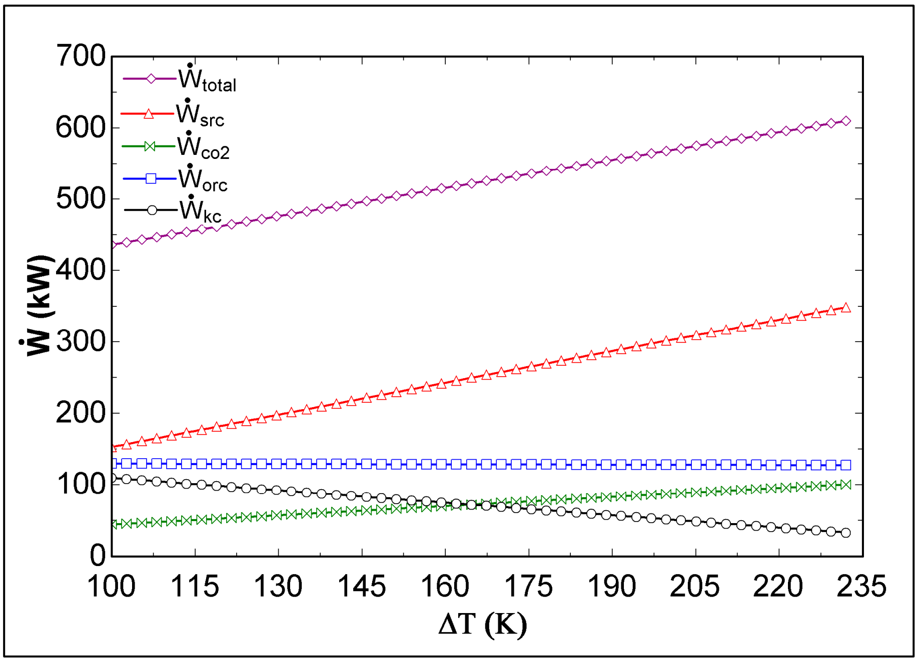

Figure 8. Change in net powers obtained with varying temperature difference.

Figure 9 gives the electrical energy cost of the entire system according to the change in SRC inlet temperature. Accordingly, electricity generation cost reaches its minimum value when the temperature change is 221.6 K and then rises again rapidly. Thus, the cost of electricity production at 221.6 K is $0.1972 per kWh. Considering that amount of energy is produced from waste heat, the competitive potential of this value in the market is quite high. For instance household electricity prices in 2023 changed by 0.32 and 0.52 $/kWh across Europe [31].

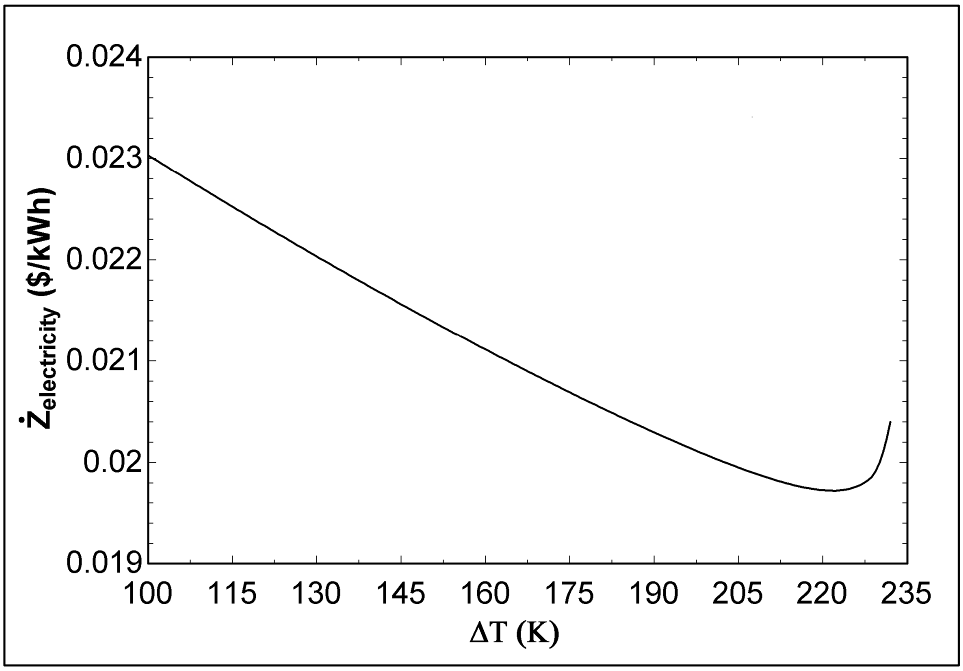

Figure 9. Electricity cost according to SRC inlet temperatures.

The efficiency of the system determines how much CO_2 is released when fuel is utilized to generate energy. For example, 23.16 tons of CO_2 emissions per day would have been discharged into the atmosphere if electricity from a 30% efficient SRC had been received from a coal power station. Therefore, we also avoid the large quantity of CO_2 emissions discharged into the environment and help to safeguard the climate by transferring waste energy using multiple heat recovery options to other integrated systems.

Figure 10 shows the PEC distributions within the cycle's total investment cost. Accordingly, PEC values of SRC, CO_2 Cycle, ORC, and KC are observed to be $312,866, $50,971, $189,961, and $140,994 respectively. Here we clearly observe that the maximum expense is SRC, and the minimum one is CO_2 cycle. Figures 9 and 10 together show that the increasing inlet temperature difference in SRC directly affects the cost of SRC and that the cost of electricity production is inversely proportional.

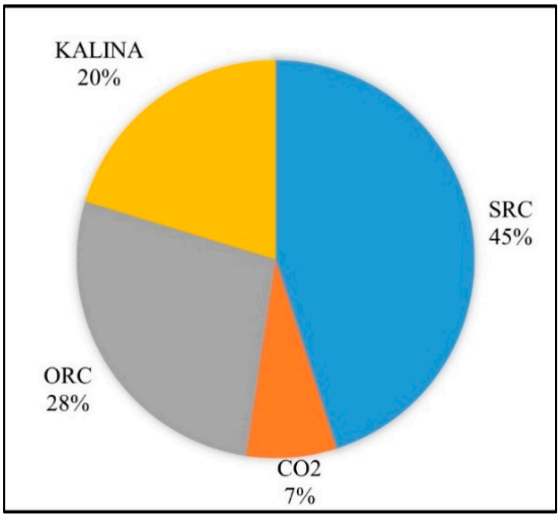

Figure 10. PEC distribution of the cycles.

When looking at the verification of this study, it can be seen that the results obtained are compatible with the literature in terms of total thermal efficiency. For example, Köse et al. [18] found an overall thermal efficiency for SRC and ORC systems used as a bottoming system in a GT-based triple combined system of 22.6%; Lu et al. [11] for municipal solid waste (MSW) as fuel combustion for power generation, 20.49%; and Ghaffarpour et al. [32] for a novel combined biomass-based power generation system, 22%.

4. Conclusions

This study examines the techno-economic aspects of recovering waste heat from an industrial AF that is emitted into the environment via the use of several integrated systems. Additionally, heat recovery's environmental impact was discussed. Utilizing four distinct integrated systems, the waste heat at 1093.15 K was assessed. To achieve maximum power generation, a parametric investigation was conducted on the SRC input temperature of the suggested system. The study's findings led to an evaluation of the systems' net output power and thermal efficiency. Consequently,

- When the SRC is investigated, the maximum net thermal efficiency of the combined system is calculated as 0.34 at 150 bar and 1146 K, respectively. In addition, maximum net power was observed as 429.83 kW.
- One of the main contributions of this study is the reduction of CO_2 emissions. In summary, the use of these combined systems is directly influential in reducing global warming.
- When the ORC is investigated, the maximum net thermal efficiency is calculated as 0.14 at 90 bar and 632.5 K, respectively. In addition, maximum net power was seen as 127.6 kW.
- The optimum value for the SRC inlet temperature difference is 221.6 K. At this point, the thermal efficiency and total power of the proposed system are 0.19 and 596.6 kW, respectively. In addition, the minimum electricity generation cost value for the proposed system is $0.1972 per kWh.

Author Contributions: Conceptualization, B.B. and E.K..; Methodology, B.B. and E.K.; Software, B.B. and E.K.; Validation, B.B., J.K. and E.K.; Formal analysis, W.T. and A.A. (Abdulrazzak Akroot); Resources, A.A. (Ali Alfaris) and Y.H.A.; Data curation, M.Y.N. and M.B.; Writing—original draft, B.B.; Writing—review and editing, E.K. and A.A. (Abdulrazzak Akroot). All authors have read and agreed to the published version of the manuscript.

Funding: This research received no external funding.

Institutional Review Board Statement: Not Applicable.

Informed Consent Statement: Not Applicable.

Data Availability Statement: The data presented in this study are available on request for confidentiality reasons from the corresponding author. The data are not publicly available due to participants of this study did not agree for their data to be shared publicly.

Acknowledgments: All the authors are grateful to Karabuk University for providing its software and hardware infrastructure to realize the current study.

Conflicts of Interest: The authors declare no conflicts of interest.

Nomenclature

A	heat transfer surface area, [m^2]
Cp	specific heat, [kJ/kgK]
CRF	capital recovery factor, [-]
KC	Kalina cycle
N	annual operating hours, [h]
n	system lifetime, [y]

ORC	organic Rankine cycle
SRC	steam Rankine cycle
PEC	purchase equipment cost, [$]
$\dot{Z}$	capital cost rate, [$/s]
Greek letters	
η	efficiency [-]
ε	effectiveness, [-]
ί	annual interest rate, [%]
ρ	density, [kg/m^3]
ϕ	maintenance factor, [-]
Subscripts	
fg	flue gas
cc	combined cycle
p	pump
t	turbine
hx	heat exchanger
cw	cooling water
gen	generator
cond	condenser
eva	evaporator
ST	steam turbine

References

1. Wang, Z.; Hu, Y.; Xia, X.; Zuo, Q.; Zhao, B.; Li, Z. Thermo-Economic Selection Criteria of Working Fluid Used in Dual-Loop ORC for Engine Waste Heat Recovery by Multi-Objective Optimization. *Energy* **2020**, *197*, 117053. [CrossRef]
2. Çalhan, R.; Kaskun Ergani, S. The Impacts of Nano Fuels Containing Fe-Ni-TiO_2/Activated Carbon Nanoparticles on Diesel Engine Performance and Emission Characteristics. *Biofuels* **2023**, *14*, 661–671. [CrossRef]
3. Zhao, J.; Ma, L.; Zayed, M.E.; Elsheikh, A.H.; Li, W.; Yan, Q.; Wang, J. Industrial Reheating Furnaces: A Review of Energy Efficiency Assessments, Waste Heat Recovery Potentials, Heating Process Characteristics and Perspectives for Steel Industry. *Process Saf. Environ. Prot.* **2021**, *147*, 1209–1228. [CrossRef]
4. Su, Z.; Zhang, M.; Xu, P.; Zhao, Z.; Wang, Z.; Huang, H.; Ouyang, T. Opportunities and Strategies for Multigrade Waste Heat Utilization in Various Industries: A Recent Review. *Energy Convers. Manag.* **2021**, *229*, 113769. [CrossRef]
5. Loni, R.; Najafi, G.; Bellos, E.; Rajaee, F.; Said, Z.; Mazlan, M. A Review of Industrial Waste Heat Recovery System for Power Generation with Organic Rankine Cycle: Recent Challenges and Future Outlook. *J. Clean. Prod.* **2021**, *287*, 125070. [CrossRef]
6. Bdaiwi, M.; Akroot, A.; Abdul Wahhab, H.A.; Assaf, Y.H.; Nawaf, M.Y.; Talal, W. Enhancement Heat Exchanger Performance by Insert Dimple Surface Ball inside Tubes: A Review. *Results Eng.* **2023**, *19*, 101323. [CrossRef]
7. Zhang, Q.; Ogren, R.M.; Kong, S.C. Thermo-Economic Analysis and Multi-Objective Optimization of a Novel Waste Heat Recovery System with a Transcritical CO_2 Cycle for Offshore Gas Turbine Application. *Energy Convers. Manag.* **2018**, *172*, 212–227. [CrossRef]
8. Kareem, A.F.; Akroot, A.; Wahhab HA, A.; Talal, W.; Ghazal, R.M.; Alfaris, A. Exergo—Economic and Parametric Analysis of Waste Heat Recovery from Taji Gas Turbines Power Plant Using Rankine Cycle and Organic Rankine Cycle. *Sustainability* **2023**, *15*, 9376. [CrossRef]
9. Liu, X.; Nguyen, M.Q.; Chu, J.; Lan, T.; He, M. A Novel Waste Heat Recovery System Combing Steam Rankine Cycle and Organic Rankine Cycle for Marine Engine. *J. Clean. Prod.* **2020**, *265*, 121502. [CrossRef]
10. Ozcan, H.; Kayabasi, E. Thermodynamic and Economic Analysis of a Synthetic Fuel Production Plant via CO_2 Hydrogenation Using Waste Heat from an Iron-Steel Facility. *Energy Convers. Manag.* **2021**, *236*, 114074. [CrossRef]
11. Lu, F.; Zhu, Y.; Pan, M.; Li, C.; Yin, J.; Huang, F. Thermodynamic, Economic, and Environmental Analysis of New Combined Power and Space Cooling System for Waste Heat Recovery in Waste-to-Energy Plant. *Energy Convers. Manag.* **2020**, *226*, 113511. [CrossRef]
12. Ishaq, H.; Dincer, I.; Naterer, G.F. Industrial Heat Recovery from a Steel Furnace for the Cogeneration of Electricity and Hydrogen with the Copper-Chlorine Cycle. *Energy Convers. Manag.* **2018**, *171*, 384–397. [CrossRef]
13. Ma, G.Y.; Cai, J.J.; Zeng, W.W.; Dong, H. Analytical Research on Waste Heat Recovery and Utilization of China's Iron & Steel Industry. *Energy Procedia* **2012**, *14*, 1022–1028. [CrossRef]
14. Zhang, Q.; Zhao, X.; Lu, H.; Ni, T.; Li, Y. Waste Energy Recovery and Energy Efficiency Improvement in China's Iron and Steel Industry. *Appl. Energy* **2017**, *191*, 502–520. [CrossRef]
15. Kumar Singh, S.; Kumar Tiwari, A.; Paliwal, H.K. Techno-Economic Assessment of Retrofitted Parabolic Trough Collector for Kalina Power Cycle. *Appl. Therm. Eng.* **2024**, *236*, 121550. [CrossRef]

16. Pan, M.; Zhu, Y.; Bian, X.; Liang, Y.; Lu, F.; Ban, Z. Theoretical Analysis and Comparison on Supercritical CO_2 Based Combined Cycles for Waste Heat Recovery of Engine. *Energy Convers. Manag.* **2020**, *219*, 113049. [CrossRef]
17. Mohammadi, K.; McGowan, J.G. Thermodynamic Analysis of Hybrid Cycles Based on a Regenerative Steam Rankine Cycle for Cogeneration and Trigeneration. *Energy Convers. Manag.* **2018**, *158*, 460–475. [CrossRef]
18. Köse, Ö.; Koç, Y.; Yağlı, H. Performance Improvement of the Bottoming Steam Rankine Cycle (SRC) and Organic Rankine Cycle (ORC) Systems for a Triple Combined System Using Gas Turbine (GT) as Topping Cycle. *Energy Convers. Manag.* **2020**, *211*, 112745. [CrossRef]
19. Ayou, D.S.; Eveloy, V. Energy, Exergy and Exergoeconomic Analysis of an Ultra Low-Grade Heat-Driven Ammonia-Water Combined Absorption Power-Cooling Cycle for District Space Cooling, Sub-Zero Refrigeration, Power and LNG Regasification. *Energy Convers. Manag.* **2020**, *213*, 112790. [CrossRef]
20. Bahrampoury, R.; Behbahaninia, A. Thermodynamic Optimization and Thermoeconomic Analysis of Four Double Pressure Kalina Cycles Driven from Kalina Cycle System 11. *Energy Convers. Manag.* **2017**, *152*, 110–123. [CrossRef]
21. Khanmohammadi, S.; Goodarzi, M.; Khanmohammadi, S.; Ganjehsarabi, H. Thermoeconomic Modeling and Multi-Objective Evolutionary-Based Optimization of a Modified Transcritical CO_2 Refrigeration Cycle. *Energy Convers. Manag.* **2018**, *5*, 86–96. [CrossRef]
22. Nazari, N.; Heidarnejad, P.; Porkhial, S. Multi-Objective Optimization of a Combined Steam-Organic Rankine Cycle Based on Exergy and Exergo-Economic Analysis for Waste Heat Recovery Application. *Energy Convers. Manag.* **2016**, *127*, 366–379. [CrossRef]
23. Wang, L.; Bu, X.; Li, H. Multi-Objective Optimization and off-Design Evaluation of Organic Rankine Cycle (ORC) for Low-Grade Waste Heat Recovery. *Energy* **2020**, *203*, 117809. [CrossRef]
24. Wang, X.; Dai, Y. Exergoeconomic Analysis of Utilizing the Transcritical CO_2 Cycle and the ORC for a Recompression Supercritical CO_2 Cycle Waste Heat Recovery: A Comparative Study. *Appl. Energy* **2016**, *170*, 193–207. [CrossRef]
25. Rivera-Tinoco, R.; Farran, M.; Bouallou, C.; Auprêtre, F.; Valentin, S.; Millet, P.; Ngameni, J.R. Investigation of Power-to-Methanol Processes Coupling Electrolytic Hydrogen Production and Catalytic CO_2 Reduction. *Int. J. Hydrogen Energy* **2016**, *41*, 4546–4559. [CrossRef]
26. IPCC. *Revised 1996 IPCC Guidelines for National Greenhouse Gas Inventories: Reference Manual*; IPCC: Geneva, Switzerland, 1996; Volume 2, pp. 21–40.
27. Wang, G.B.; Zhang, X.R. Thermoeconomic Optimization and Comparison of the Simple Single-Stage Transcritical Carbon Dioxide Vapor Compression Cycle with Different Subcooling Methods for District Heating and Cooling. *Energy Convers. Manag.* **2019**, *185*, 740–757. [CrossRef]
28. Emadi, M.A.; Chitgar, N.; Oyewunmi, O.A.; Markides, C.N. Working-Fluid Selection and Thermoeconomic Optimisation of a Combined Cycle Cogeneration Dual-Loop Organic Rankine Cycle (ORC) System for Solid Oxide Fuel Cell (SOFC) Waste-Heat Recovery. *Appl. Energy* **2020**, *261*, 114384. [CrossRef]
29. Seyyedvalilu, M.H.; Zare, V.; Mohammadkhani, F. Comparative Thermoeconomic Analysis of Trigeneration Systems Based on Absorption Heat Transformers for Utilizing Low-Temperature Geothermal Energy. *Energy* **2021**, *224*, 120175. [CrossRef]
30. Sohrabi, A.; Asgari, N.; Imran, M.; Wakil Shahzad, M. Comparative Energy, Exergy, Economic, and Environmental (4E) Analysis and Optimization of Two High-Temperature Kalina Cycles Integrated with Thermoelectric Generators for Waste Heat Recovery from a Diesel Engine. *Energy Convers. Manag.* **2023**, *291*, 117320. [CrossRef]
31. Statista. Household Electricity Prices Worldwide in June 2023, by Select Country. Available online: https://www.statista.com/statistics/263492/electricity-prices-in-selected-countries/ (accessed on 5 March 2024).
32. Ghaffarpour, Z.; Mahmoudi, M.; Mosaffa, A.H.; Garousi Farshi, L. Thermoeconomic Assessment of a Novel Integrated Biomass Based Power Generation System Including Gas Turbine Cycle, Solid Oxide Fuel Cell and Rankine Cycle. *Energy Convers. Manag.* **2018**, *161*, 1–12. [CrossRef]